Empirical tight binding parameters for GaAs and MgO with explicit basis through DFT mapping

Yaohua Tan, Michael Povolotskyi, Tillmann Kubis, Yu He, Zhengping Jiang and Gerhard Klimeck

School of Electrical and Computer Engineering,Network for Computational Nanotechnology,Purdue University, West Lafayette, Indiana,USA,47906

Timothy B. Boykin

University of Alabama in Huntsville,Huntsville, Alabama 35899 USA

Abstract. The Empirical Tight Binding(ETB) method is widely used in atomistic device simulations. The reliability of such simulations depends very strongly on the choice of basis sets and the ETB parameters. The traditional way of obtaining the ETB parameters is by fitting to experiment data, or critical theoretical bandedges and symmetries rather than a foundational mapping. A further shortcoming of traditional ETB is the lack of an explicit basis. In this work, a DFT mapping process which constructs TB parameters and explicit basis from DFT calculations is developed. The method is applied to two materials: GaAs and MgO. Compared with the existing TB parameters, the GaAs parameters by DFT mapping show better agreement with the DFT results in bulk band structure calculations and lead to different indirect valleys when applied to nanowire calculations. The MgO TB parameters and TB basis functions are also obtained through the DFT mapping process.

Modern semiconductor nanodevices have reached critical device dimensions in the range of several nanometers. These devices consist of complicated two and three dimensional geometries composed of multiple materials. Typically, about 10000 to 10 million atoms are in the active device region with contacts controlling the current injection. This finite extent suggests an atomistic, local and orbital-based electronic structure representation. Quantitative device design requires the reliable prediction of bandgaps and band offsets within a few meV and effective masses at principal symmetry points within a few percent.

Ab-initio methods that have no adjustable parameters offer such atomistic representations. However, accurate models such as hybrid functionals [1], GW [2] and BSE approximations [3] are computationally far too expensive to be applied on multi-million atom devices. More approximate ab-initio methods such as the local density approximations (LDA) and generalized gradient approximations (GGA) [4] do not reproduce band gaps, relative band offsets, and effective masses accurately enough. Empirical methods such as the empirical tight binding (ETB) method are numerically much more efficient. The accuracy of ETB is hereby limited by the parameters fitting. Previous ETB simulations in semiconductor nanodevices such as resonant tunneling diodes [5], quantum dots [6] and strained Si/SiGe quantum wells [7] showed quantitative agreement with experiments.

The accuracy of the ETB method depends critically on the careful calibration of the empirical parameters. The common way to determine the ETB parameters is to fit ETB results to experimental band structures [8] [9]. One shortcoming of this method is its requirement of experimental data that are often not available for new and exotic materials. In addition, the ETB basis functions remain unknown, which makes it notoriously difficult to predict wave function dependent quantities with high precission. To overcome these shortcomings, some approaches were developed to construct localized basis functions from ab-initio results such as localized wannier functions [10] or quasi-atomic orbitals [11] [12] [13]. Unfortunately, these functions are either not reliably centered at atoms, or resulting Hamiltonian requires long distance coupling with large number of neighbors, which is numerically expensive. Nanoelectronic devices are increasingly based on complex heterstructures in 1 or 2 dimensions including atomistc disorder and strain. In this realm models with one or two neighbors are conceptually preferrable and simple to implement. In contrast the validity of many neighbor bulk basis states are very questionable in this domain.

In this work, a DFT mapping method that constructs ETB parameters from ab-initio calculations is presented. This method allows to determine ETB basis functions that are centered at atoms and it limits the interatomic coupling to the first or second nearest neighbors. Since the method does not require experimental results, the ETB parameters are less empirical. Two materials are considered in this work: 1) the well known GaAs to validate the method and 2) MgO which is recently used as a magnetic tunneling barrier material in Magnetoresistive Random-Access-Memory devices. MgO lacks the elaborate experimental analysis, but it is known to have small spin-orbit

interaction and a large band gap [14].

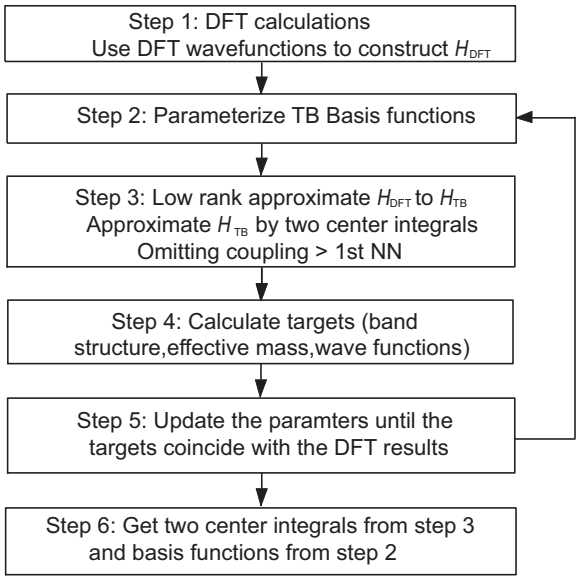

Figure 1. The process of TB parameters construction from DFT calculations.

Figure 1 shows the flow chart of the mapping method. The first step is to perform ab-initio calculations of the band structure of a material. In general, any method that is capable to calculate electronic band structures and wave functions is suitable here. However, in this work, DFT calculations including hybrid functionals corrections for 60 electronic bands performed with VASP version 5.2 [15] are used. Inthe second step, the ETB basis functions for each type of atom are defined as

$$\Psi_{n,l,m}(\mathbf{r}) \equiv \Psi_{n,l,m}(r,\theta,\phi) = R_{n,l}(r)\, Y_{l,m}(\theta,\phi), \tag{1}$$

where the functions $Y_{l,m}$ are the complex spherical harmonics and the functions $R_{n,l}$ are exponentially damped plane waves

$$R_{n,l}(r) = \sum_{i=1}^{N} \left[a_i \sin(\lambda_i r) + b_i \cos(\lambda_i r)\right] r^{n-1} \exp(-\alpha_i r). \tag{2}$$

Here, $\mathbf{r} = (r,\theta,\phi)$ is the position vector with the respective atom centered at the origin, l, m are the angular and magnetic quantum numbers of the orbital basis function, and n is the principal number of the atomic orbital as used in Hückel type basis functions [16]. The remaining parameters $a_i, b_i, \alpha_i, \lambda_i$ are the fitting parameters. The ETB basis functions are spin independent. With a given set of ETB basis functions $\Psi^{\mathbf{k}}_{TB}$, in the third step, a transformation matrix between these chosen DFT basis functions $\psi^{\mathbf{k}}_{\mathrm{DFT}}$ and the $\Psi^{\mathbf{k}}_{\mathrm{TB}}$ is calculated. Since the number of the ETB basis functions is smaller than the DFT basis funcitons, this transformation matrix is rectangular and represents a low rank approximation. [17] Then, the DFT Hamiltonian is transformed to the tight binding representation. The ETB Hamilton matrix elements are approximated by two center integrals according to the Slater-Koster table [18] [19]. Any non-zero off-diagonal element of the overlap matrix is neglected. ETB Hamilton matrix elements

beyond either 1st or 2nd nearest neighbor coupling are neglected. In Step 4, the band edges, effective masses and eigen functions of the Hamiltonian at high symmetry points are calculated and compared to the corresponding DFT results. The overlaps of the ETB basis functions are also determined. In the fifth step, all fitting parameters are adjusted to improve 1) the agreement of the ETB results with the DFT ones and 2) reduce the overlap matrix of the ETB basis functions to the unity matrix. Steps 2 - 5 are repeated until the convergence criterion is met, i.e. when the maximum difference of DFT and ETB band edges are within 10 meV, when the effective masses agree within 5% and when the eigenfunctions of DFT and ETB calculations agree by at least 90%. Step 6 requires to extract the converged ETB basis functions and the ETB two center integrals.

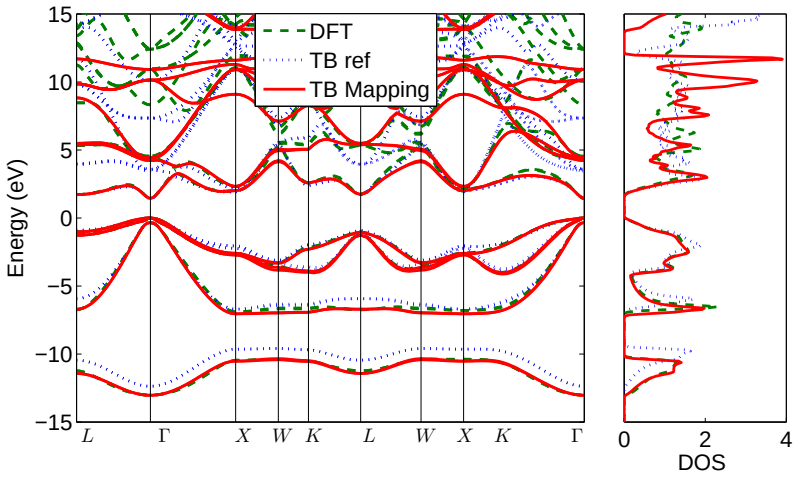

Figure 2. Band structure and density of states of GaAs by DFT(green dashed lines), TB using parameters in ref[9] and TB using parameters by this work.

For GaAs and MgO, eigenfunctions and eigen energies of the lowest 16 bands of the DFT calculations from L to Γ and Γ to X are taken into account for the ETB fitting method. Here, the wave functions for the topmost valence bands and lowest conduction band valley are considered in the fitting of ETB eigenfunctions to the DFT ones. The overlap of the ETB basis functions is partly minimized in the fitting process. Most of the overlap matrix elements vanish, but the maximum overlap i.e. in this case the overlap of the p orbitals of cations and d orbitals of anions, e.g. $\langle p_x^{Ga} | d_{yz}^{As} \rangle = 0.86$ at the Γ point remains comparably high. GaAs is parameterized for the 1st nearest neighbor $sp^3d^5s^*$ ETB model. The resulting parameters can be found in table 2. The band structure and density of states of GaAs are shown in Fig. 2. Calculated bandstructures of the DFT method, of the ETB method with parameters of the present mapping method and of the ETB method with previously published parameters [9] are compared in Fig. 2 as well. The ETB calculations with new parameters agree very well with the DFT results for energies below 5 eV whereas ETB calculations with previously published parameters deviate from the DFT results already at about 2 eV. Relevant band edges and effective

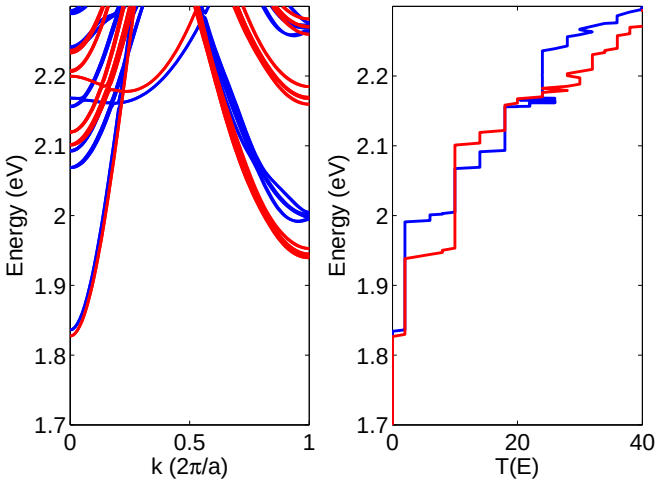

Figure 3. Comparison of E-k diagram of conduction bands (left figure) and Transmission (right figure) of GaAs nanowire . The red lines are results using TB parameters generated by this work; the blue line are results using TB parameters by ref[9].

	GaAs				MgO		
Quantity	DFT	TB	Error	ref[9]	DFT	TB	Error
$E_g(\Gamma)$	1.420	1.449	2.96%	1.413	7.831	7.499	4.2%
$E_g(X)$	1.973	1.947	0.9%	1.898	12.161	11.819	2.8%
$E_g(L)$	1.728	1.718	0.6%	1.714	10.871	10.469	3.7%
m^*_Γ	0.0692	0.0737	6.5%	0.0657	0.396	0.458	15.6%
$m^*_{(X,l)}$	1.140	1.117	2.0%	1.881	–	–	–
$m^*_{(X,t)}$	0.219	0.231	5.5%	0.175	–	–	–
$m^*_{(L,l)}$	1.700	1.756	3.3%	1.728	–	–	–
$m^*_{(L,t)}$	0.133	0.138	3.8%	0.098	–	–	–
γ_1	6.964	6.985	1.1%	7.388	0.952	0.889	6.6%
γ_2	2.084	2.151	3.6%	2.367	0.277	0.219	20.9%
γ_3	2.972	2.980	1.1%	3.098	0.376	0.234	37.7%

Table 1. Comparison of important bandedges and effective masses of GaAs and MgO by DFT and TB.

masses are compared in table 1, demonstrating a much better fit.

Figure 3 compares results of ETB calculations of the band structure and the transmission coefficient of a GaAs 3.5 nm $\times$ 3.5 nm squared nanowire when the new and the previously published parameter set are used. The results agree for the Γ point at lower energies, but they deviate significantly for the indirect conduction valley at about 1.9 eV. The difference in the confinement energy of this conduction valley originates from different transverse effective masses at the L point of the two ETB parameter sets (see Table 1). The modeling go the details of the high symmetry points is particularly

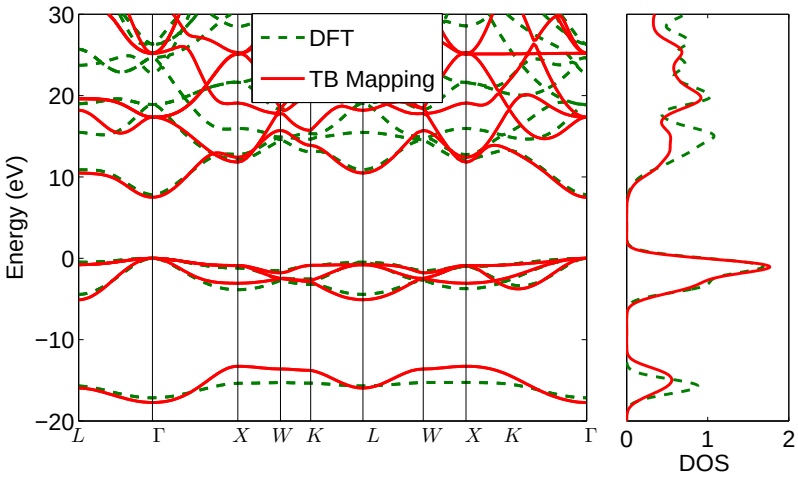

Figure 4. Band structure and density of states of MgO by DFT and TB.

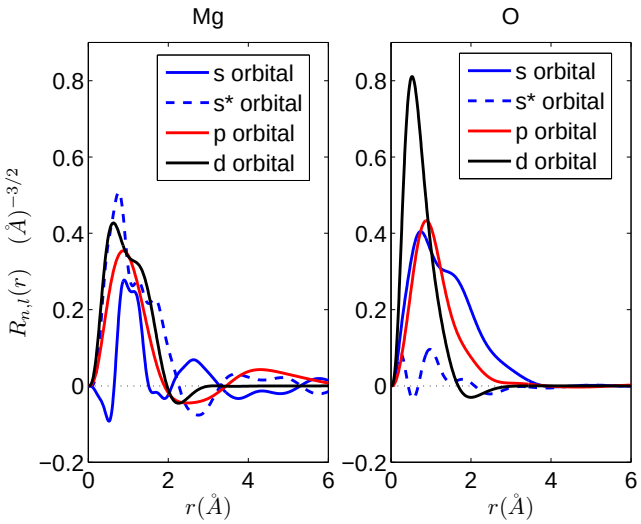

Figure 5. Radial part of Basis functions of Mg and O atoms in MgO.

important for the emerging concept of gamma-L transistors [20].

MgO cyrstalizes in Rocksalt structure. Each Oxygen atom has 6 Magnesium atoms as 1st nearest neighbors and 12 Oxygen atoms as 2nd nearest neighbors. The valence bands of MgO are formed by hybridized orbitals of Oxygen atoms: The s-orbitals and p-orbitals of Oxygen contribute to valence bands around -17 eV and -1 eV respectively, while the s^*, d-orbitals of Oxygen and orbitals of Magnesium contribute to the band structure for energies beyond 7 eV (see Fig. 4). According to this, MgO is parameterized for a 2nd nearest neighbor $sp^3d^5s^*$ ETB model (for parameters see table 3). Within this model, the interaction between two Oxygen atoms is required to produce the correct valence bands. The interaction between two Magnesium atoms is omitted, since the onsite energies of Magnesium orbitals are higher than 20 eV so that the omission will only affect bands close to that high and technically irrelevant energy. The ETB band

structure matches the DFT result well within the energies 5 to 20 eV. Important band properties calculated in the DFT and the ETB method are listed in Table 1. The basis functions of Oxygen and Magnesium are shown in Fig. 5. The basis functions of Oxygen are more localized while the basis functions of Magnesium are more plane wave like functions. This difference in the localization originates from the fact that Magnesium orbital energies are higher than the Oxygen ones.

In conclusion, a method to determine ETB parameters from density function theory calculations is developed. The method is applied to GaAs and MgO. First nearest neighbor ETB parameters and basis functions for an $sp^3d^5s^*$ model of GaAs are presented. Results of this parameterization agree well with the DFT calculations. The new ETB parameters lead to lower indirect conduction bands when applied to GaAs nanowires. Second nearest neighbor ETB parameters and basis functions for an $sp^3d^5s^*$ model of MgO are also obtained. The ETB results with this parameterization also agree well with the DFT calculations.

nanoHUB.org computational resources operated by the Network for Computational Nanotechnology funded by NSF are utilized in this work. The research was funded by the Lockheed Martin Corporation and NSF (Award No. 1125017)

Table 2. Tight Binding Parameters for bulk GaAs

Parameter	value	Parameter	value
E_{sa}	-4.5863	$s_a^*p_c\sigma$	2.6877
E_{pa}	1.4694	$s_c^*p_a\sigma$	1.8335
E_{s*a}	10.0480	$s_ad_c\sigma$	-2.1172
E_{da}	11.2878	$s_cd_a\sigma$	-2.9128
E_{sc}	-1.3323	$s_a^*d_c\sigma$	-0.4974
E_{pc}	9.5885	$s_c^*d_a\sigma$	-2.9971
E_{s*c}	25.6752	$pp\sigma$	3.8065
E_{dc}	35.2863	$pp\pi$	-1.5010
Δ_a	0.1259	$p_ad_c\sigma$	-1.2077
Δ_c	0.1235	$p_cd_a\sigma$	-1.9855
$ss\sigma$	-1.7615	$p_ad_c\pi$	3.1547
$s^*s^*\sigma$	-0.8374	$p_cd_a\pi$	2.3234
$s_a^*s_c\sigma$	-1.1173	$dd\sigma$	-1.9986
$s_as_c^*\sigma$	-2.9313	$dd\pi$	3.1681
$s_ap_c\sigma$	2.1768	$dd\delta$	-2.3137
$s_cp_a\sigma$	3.6705		

Table 3. Tight Binding Parameters for bulk MgO

Parameter	Value	Parameter	Value
E_{sa}	-7.1496	$p_a d_c \pi$	1.5284
E_{pa}	5.8926	$p_c d_a \pi$	-4.0453
E_{s*a}	23.8138	$d_a d_c \sigma$	-1.0038
E_{da}	40.0285	$d_a d_c \pi$	5.0830
E_{sc}	38.4754	$d_a d_c \delta$	-0.6323
E_{pc}	32.1465	$s_a s_a \sigma$	-0.2718
E_{s*c}	45.5084	$s_a^* s_a^* \sigma$	-0.4690
E_{dc}	57.9865	$s_a s_a^* \sigma$	-0.0001
Δ_a	0.0031	$s_a p_a \sigma$	0.3388
Δ_c	0.0298	$s_a^* p_a \sigma$	0.1965
$s_a s_c \sigma$	-0.1192	$s_a d_a \sigma$	-0.3380
$s_a^* s_c^* \sigma$	1.6477	$s_a^* d_a \sigma$	-0.4407
$s_a^* s_c \sigma$	-0.6008	$p_a p_a \sigma$	0.4371
$s_a s_c^* \sigma$	-0.6347	$p_a p_a \pi$	-0.0641
$s_a p_c \sigma$	-2.0013	$p_a d_a \sigma$	-0.4039
$s_c p_a \sigma$	0.3283	$p_a d_a \pi$	0.6986
$s_a^* p_c \sigma$	2.1584	$d_a d_a \sigma$	-2.3768
$s_c^* p_a \sigma$	2.1282	$d_a d_a \pi$	0.4556
$s_a d_c \sigma$	0.6641	$d_a d_a \delta$	0.0967
$s_c d_a \sigma$	-2.9483		
$s_a^* d_c \sigma$	1.6890		
$s_c^* d_a \sigma$	3.1534		
$p_a p_c \sigma$	0.1743		
$p_a p_c \pi$	-0.4703		
$p_a d_c \sigma$	-1.9960		
$p_c d_a \sigma$	0.0519		

References

[1] A. Krukau, O. Vydrov, A. Izmaylov, and G. Scuseria, J. Chem. Phys. **124**, 224106 (2006).
[2] M. S. Hybertsen and S. G. Louie, Phys. Rev. B **34**, 5390 (1986).
[3] S. Ismail-Beigi and S. G. Louie, Phys. Rev. Lett. **90**, 076401 (2003).
[4] M. C. Payne, M. P. Teter, D. C. Allan, T. A. Arias, and J. D. Joannopoulos, Rev. Mod. Phys. **64**, 1045 (1992).
[5] R. Lake, G. Klimeck, and S. Datta, Phys. Rev. B **47**, 6427 (1993).
[6] G. Klimeck, F. Oyafuso, T. B. Boykin, C. R. Bowen, and P. V. Allmen, Computer Modeling in Engineering and Science (CMES) **3**, 601 (2002).
[7] T. B. Boykin, G. Klimeck, M. Eriksson, M. Friesen, S. Coppersmith, P. Allmen, F. Oyafuso, and S. Lee, Applied Physics Letter **84**, 115 (2004).
[8] J.-M. Jancu, R. Scholz, F. Beltram, and F. Bassani, Phys. Rev. B **57**, 6493 (1998).
[9] T. B. Boykin, G. Klimeck, R. C. Bowen, and F. Oyafuso, Phys. Rev. B **66**, 125207 (2002).
[10] N. Marzari and D. Vanderbilt, Phys. Rev. B **56**, 12847 (1997).

[11] X. Qian, J. Li, L. Qi, C.-Z. Wang, T.-L. Chan, Y.-X. Yao, K.-M. Ho, and S. Yip, Phys. Rev. B **78**, 245112 (2008).
[12] W. C. Lu, C. Z. Wang, T. L. Chan, K. Ruedenberg, and K. M. Ho, Phys. Rev. B **70**, 041101 (2004).
[13] A. Urban, M. Reese, M. Mrovec, C. Elsässer, and B. Meyer, Phys. Rev. B **84**, 155119 (2011).
[14] S. Yuasa, T. Nagahama, A. Fukushima, Y. Suzuki, and K. Ando, Nature Materials **3**, 868 (2004).
[15] Y.S. Kim, K. Hummer, and G. Kresse, Phys. Rev. B **80**, 035203 (2009).
[16] J. Cerdá and F. Soria, Phys. Rev. B **61**, 7965 (2000).
[17] https : //en.wikipedia.org/wiki/Low-rank_approximation
[18] J. C. Slater and G. F. Koster, Phys. Rev. **94**, 1498 (1954).
[19] A. V. Podolskiy and P. Vogl, Phys. Rev. B **69**, 233101 (2004).
[20] M. Rodwell, M. Frensley, S. Steiger, E. Chagarov, S. Lee, H. Ryu, Y. Tan, L. Wang, J. Law, T. Boykin, et al., Device Research Conference (DRC) p. 149 (2010).